Eur. Phys. J. D **46**, 89–92 (2008)
DOI: 10.1140/epjd/e2007-00314-3

THE EUROPEAN PHYSICAL JOURNAL D

Antiproton and proton energy loss straggling at keV energies

S.P. Møller[1], A. Csete[2], T. Ichioka[2], H. Knudsen[2], H.-P.E. Kristiansen[2], U.I. Uggerhøj[2,a], H.H. Andersen[3], P. Sigmund[4], and A. Schinner[5]

[1] Institute for Storage Ring Facilities, University of Aarhus, 8000 Aarhus C, Denmark
[2] Department of Physics and Astronomy, University of Aarhus, 8000 Aarhus C, Denmark
[3] Ørsted Laboratory, Niels Bohr Institute, Universitetsparken 5, 2100 København Ø, Denmark
[4] Department of Physics and Chemistry, University of Southern Denmark, Campusvej 55, 5230 Odense M, Denmark
[5] Institut für Experimentalphysik, Johannes-Kepler-Universität, 4040 Linz-Auhof, Austria

Received 13 August 2007
Published online 23 November 2007 –

Abstract. The slowing-down process of point-like charged particles in matter has been investigated by measuring the energy straggling for antiprotons and protons in Al, Ni and Au. A comparison with binary theory shows good agreement for Al and Au. For Ni, experimental data are not as convincing. In particular for the aluminum target, the Barkas-like effect of reduced energy straggling for antiprotons compared to protons is visible in the experimental data and a nearly velocity-proportional straggling is found, in good agreement with binary theory.

PACS. 34.50.Bw Energy loss and stopping power – 61.85.+p Channeling phenomena (blocking, energy loss, etc.)

1 Introduction

We present measurements of antiproton and proton energy loss straggling at energies 1–70 keV, derived from energy loss distributions obtained in previous measurements of stopping powers [1,2]. In fact, such measurements of straggling for antiprotons were 'promised' already in the early nineties [3], eagerly sought by theorists [4] and also in the case of protons, the area still attracts substantial interest [5–10]. In the construction of modern trapping schemes for antiprotons — in pursuit of the goal of producing cold antihydrogen or a low-energy antihydrogen beam — energy straggling of antiprotons becomes an important issue [11].

2 Energy loss and straggling

When a proton or antiproton ($\overline{\mathrm{p}}$) traverses matter, it will lose energy mainly in electronic collisions with target atoms, whereby atoms are excited or ionized. The slowing-down is mainly characterized by the stopping power $-\mathrm{d}E/\mathrm{d}x$. At low energies it is often the case that the stopping power is proportional to projectile velocity as expected from e.g. the free-electron gas approximation [12,13]. We have recently confirmed this approximation with antiproton measurements in metals [1], and surprisingly also at low energies for a large band-gap insulator, LiF [2].

However, also higher order moments of the energy loss distribution characterize the slowing-down process, most importantly the energy loss straggling $\Omega^2 = \langle(\Delta E^2 - \langle\Delta E\rangle)^2\rangle$, where ΔE is the energy loss and $\langle\Delta E\rangle$ is the mean energy loss. Already in 1915, Bohr derived an expression [14] that is quite successful in describing energy loss straggling for swift (but non-relativistic) particles penetrating a thin target of thickness Δt

$$\Omega_{\mathrm{B}}^2 = 4\pi Z_1^2 Z_2 e^4 N \Delta t \tag{1}$$

where $Z_1 e$ is the charge of the projectile nucleus, $Z_2 e$ the charge of the nuclei in the target and N the density of atoms. This formula is based on Rutherford scattering off free electrons.

The energy loss distribution is Gaussian, when energy transfers in individual collisions are small compared to the width of the final distribution. In the present experiment, this is the case for not too thin targets.

When the projectile is slower than the fast, inner-shell target electrons, the straggling is reduced relative to the Bohr value. This effect is most easily taken into account in an electron-gas model, as was done by Lindhard and Scharff [13,15] and later refined by Bonderup and Hvelplund [16]. Moreover, in the free-electron gas approximation, energy loss straggling is expected to be proportional to v^2 [4,13,16,17].

[a] e-mail: ulrik@phys.au.dk

Target inhomogeneities may contribute to the measured energy loss fluctuations. For an inhomogeneous target with a thickness variation δx, there will be an additional fluctuation in the energy loss of a transmitted beam given from [18] $\Omega_\delta^2 = (\mathrm{d}E/\mathrm{d}x)^2\delta x^2$ such that inhomogeneities may be included in the theoretical description by adding the contribution in quadrature to the energy loss straggling

$$\Omega_{\delta\mathrm{th}}^2 = \Omega_{\mathrm{th}}^2 + \Omega_\delta^2. \quad (2)$$

3 Barkas effect in straggling

Particles of negative charge are subject to a lower stopping power than positive particles due to polarization of the target electrons. This so-called Barkas effect, which was first observed as a range difference between positive and negative pions [19], has in the last decade been studied in detail with antiprotons [1,20].

Binary stopping theory developed by two of us [21,22] is a suitable scheme to calculate stopping and straggling. This non-perturbative classical theory includes Bohr's classical result for distant collisions and Rutherford's law for close collisions. It predicts stopping powers for ions very accurately in a wide range of energies [23].

A Barkas effect in straggling is present in binary theory calculations of energy loss straggling, antiproton straggling being reduced by up to a factor of 2 compared to the value for protons [9,24].

4 Experiment

The experimental procedures in the present study follow closely those described in [25]. In short, the Antiproton Decelerator at CERN delivers around 10^7 antiprotons in a pulse of 200 ns duration at a kinetic energy of 5.3 MeV with a repetition time of about 2 minutes. A Radio Frequency Quadrupole subsequently decelerates this beam to an energy that can be varied between essentially 0 and 120 keV. We note that the average beam current is extremely small and hence there is no foil deterioration during the measurements.

The experimental apparatus, see Figure 1, used in the determination of the stopping power and its fluctuations, is based on two 90° electrostatic spherical analyzers (ESA). The first analyzer is used to select an incident beam with a small energy spread around the mean energy $\langle E_1\rangle$. After traversal of the target foil of thickness Δt, a second analyzer measures exit energies of the beam, centered around $\langle E_2\rangle$. The stopping power is then determined as $-\mathrm{d}E/\mathrm{d}x = (\langle E_1\rangle - \langle E_2\rangle)/\Delta t$ at the average energy $(\langle E_1\rangle + \langle E_2\rangle)/2$. The $\overline{\mathrm{p}}$ beam is detected by two-stage channel-plate detectors with optical readout by CCD cameras from a phosphor screen. One detector is positioned after the first analyzer, for tuning of the incident beam, and another one after the second analyzer, see Figure 1. The whole setup has been thoroughly calibrated and tested using protons of known energy [1,25]. The energy loss fluctuation is determined by measuring the RMS

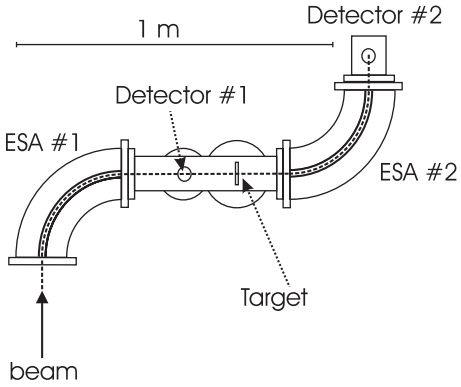

Fig. 1. Schematic diagram of the experiment. The target foil is insulated and can be raised to a bias voltage in order to vary the projectile impact energy.

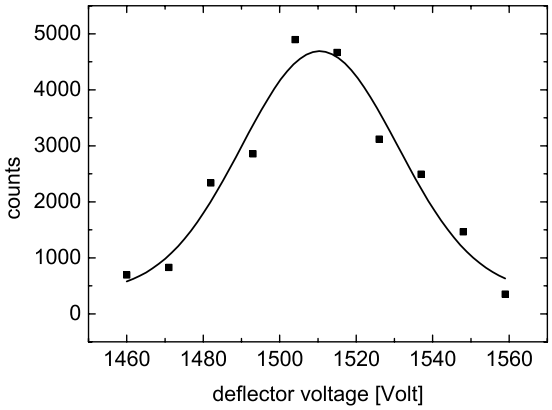

Fig. 2. Energy loss distribution for aluminum. The vertical axis is proportional to the light intensity detected by a two-stage channel-plate detector with optical readout by a CCD camera viewing a phosphor screen. The horizontal axis is the deflector voltage of the second spherical analyzer, proportional to the energy of the transmitted particles.

width, Ω, of the energy loss distribution, an example of which is shown in Figure 2.

5 Results

The measured fluctuation for the three elements used in the present experiments is shown in Figures 3–5. The values have been obtained by fitting a Gaussian distribution to the measured data as in Figure 2. In addition, an inhomogeneity contribution has been added to the theoretical values for proton straggling (dash-dotted lines) and antiproton straggling (dotted lines). This contribution has been found by addition of the inhomogeneity contribution Ω_δ in quadrature, to obtain the best fit to the data for proton impact on the foils. Since the *same* foils were used for the measurements with antiprotons, an inhomogeneity contribution based on the same target inhomogeneities must be added in quadrature to the antiproton calculations. This gives an accurate estimate of the Barkas-like difference, even in the presence of inhomogeneities.

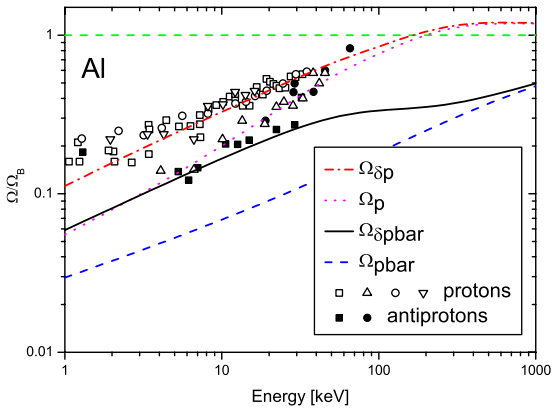

Fig. 3. Measured antiproton (■, 260 Å foil, • 350 Å) and proton (△ 260 Å, ▽ 260 Å, □ 320 Å, ◯ 320 Å) fluctuation in aluminum, normalized to the Bohr straggling Ω_B. See the text for an explanation of the curves.

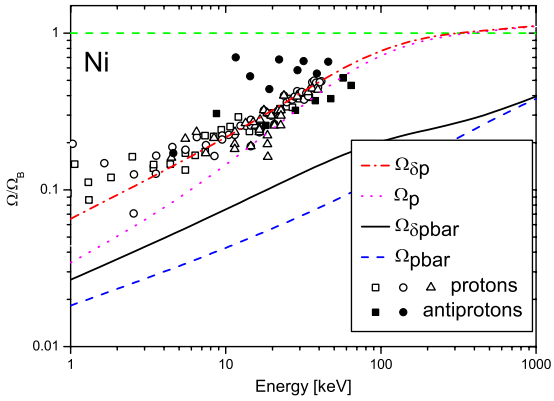

Fig. 4. Measured antiproton (■, 220 Å foil, • 220 Å) and proton (△ 220 Å, □ 220 Å, ◯ 220 Å) fluctuation in nickel, normalized to the Bohr straggling Ω_B. See the text for an explanation of the curves.

In Figures 3–5, the horizontal dashed line shows the high-energy asymptote, the Bohr value Ω_B. We observe that our data for the Al and Au targets agree fairly well with the calculations including a small thickness variation of $\delta x_{Al} = 60$Å, $\delta x_{Au} = 80$ Å.

For the aluminum data in Figure 3, the three proton data sets shown by the symbols $(\nabla, \square, \bigcirc)$ are in excellent agreement with the binary theory calculations including inhomogeneities. For the data set shown by $(\triangle)$, there is a slight, unexplained discrepancy, both with theory and with the remaining data. One possible explanation for the discrepancy is channeling. As shown in [26], even at 1.4 MeV the dechanneling of antiprotons is substantial in a 0.5 μm thick Si crystal, so any discrepancy observed for antiprotons is unlikely to be a channeling effect. On the other hand, for protons the dechanneling length is much larger and channeling through differently oriented crystallites may affect the measured fluctuation [27]. The antiproton data sets show a somewhat larger scatter than the proton data, but the tendency is clear: the energy loss fluctuations of antiprotons is generally smaller than for protons, as expected.

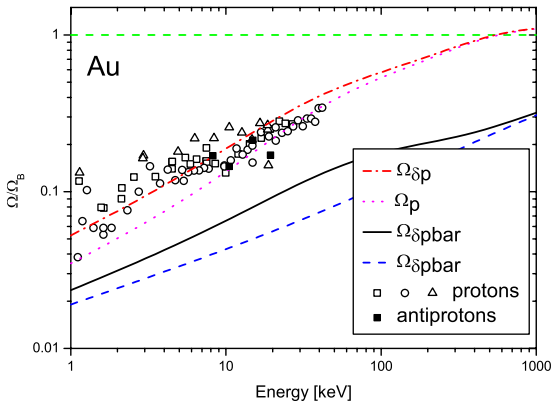

Fig. 5. Measured antiproton (■, 200 Å foil) and proton (△ 200 Å, □ 200 Å, ◯ 200 Å) fluctuation in gold, normalized to the Bohr straggling Ω_B. See the text for an explanation of the curves.

A least-squares fit to the (□) data set yields a dependence of fluctuation on velocity of the form $\Omega \propto v^{0.9\pm0.2}$, in good agreement within the uncertainty with the exponent of 1.2 found from binary theory, but significantly smaller than the v^2 proportionality found from electron gas models [4,16].

In the case of nickel, shown in Figure 4, for one data set (•) we measure a higher fluctuation for antiprotons than for protons. This is unexpected and the large scatter of points indicates that this data set — in spite of seemingly reliable Gaussian fits — is not trustworthy. The other data set (■) shows a small trend in the direction of the same conclusion as for aluminum.

Turning to the gold target, shown in Figure 5, the proton data agree quite well with the calculations, although the slope of the experimental values Ω/Ω_B seems slightly lower than the theory predicts. The measured values for antiprotons are too few to reach a firm conclusion, but there is certainly no contradiction to the Barkas-like reduction for antiprotons.

Accurate comparisons to other theories based on an electron gas model [4,28], are difficult since the electron gas model generally applies only to the conduction electrons which in turn contribute less than half to the total straggling [9].

The results presented here and in our earlier publications [1,2,25] show the usefulness of the technique of electrostatic analysis for measurements of energy loss and energy loss straggling. In one apparatus, it is possible to measure over two orders of magnitude in energy, for both protons and antiprotons. Furthermore, in principle the only limiting factor preventing measurements at energies below 1 keV is foil thickness and homogeneity. The applied technique is thus extremely versatile.

6 Conclusion

In conclusion, we have measured the fluctuations in energy loss (which includes the energy loss straggling) for antiprotons and protons in the energy range 1–70 keV, traversing

thin foils of aluminum, nickel and gold. In particular for the aluminum target, the reduced straggling of antiprotons compared to protons is visible in the data, whereas for nickel and gold the quality of the data is too poor to validate such a firm conclusion. Nevertheless, there is no contradiction with the binary theory of Sigmund and Schinner, taking into account the experimental statistical uncertainty as evaluated by the scatter of data points.

This work has been supported by the Danish Natural Science Research Council (FNU, ICEII). We also acknowledge the technical help of CERN staffs and the assistance and advice from collaborators within the ASACUSA collaboration.

References

1. S.P. Møller, A. Csete, T. Ichioka, H. Knudsen, U.I. Uggerhøj, H.H. Andersen, Phys. Rev. Lett. **88**, 193201 (2002)
2. S.P. Møller, A. Csete, T. Ichioka, H. Knudsen, U.I. Uggerhøj, H.H. Andersen, Phys. Rev. Lett. **93**, 042502 (2004)
3. S.P. Møller, Nucl. Instr. Meth. B **48**, 1 (1990)
4. I. Nagy, A. Arnau, P.M. Echenique, E. Zaremba, Phys. Rev. B **44**, 12172 (1990)
5. G. Konac, S. Kalbitzer, Ch. Klatt, D. Niemann, R. Stoll, Nucl. Instr. Meth. B **136**, 159 (1998)
6. M. Famá, J.C. Eckardt, G.H. Lantschner, N.R. Arista, Phys. Rev. Lett. **85**, 4486 (2000)
7. J.C. Eckardt, G.H. Lantschner, Nucl. Instr. Meth. B **175**, 93 (2001)
8. J.H.R. dos Santos, P.L. Grande, M. Behar, J.F. Dias, N.R. Arista, J.C. Eckhardt, G.H. Lantschner, Phys. Rev. A **68**, 042903 (2003)
9. P. Sigmund, A. Schinner, Eur. Phys. J. D **23**, 201 (2003)
10. F. Allegrini, D.J. McComas, D.T. Young, J.-J. Berthelier, J. Covinhes, J.-M. Illiano, J.-F. Riou, H.O. Funsten, R.W. Harper, Rev. Sci. Instr. **77**, 044501 (2006)
11. N. Kuroda et al., Phys. Rev. Lett. **94**, 023401 (2005)
12. E. Fermi, E. Teller, Phys. Rev. **72**, 399 (1947)
13. J. Lindhard, K. Dan. Vidensk. Selsk. Mat.-Fys. Medd. **28**, (1954)
14. N. Bohr, Phil. Mag. **30**, 581 (1915)
15. J. Lindhard, M. Scharff, Mat. Fys. Medd. Dan. Vid. Selsk. **27**, 15 (1953)
16. E. Bonderup, P. Hvelplund, Phys. Rev. A **4**, 562 (1971)
17. W.K. Chu, Phys. Rev. A **13**, 2057 (1976)
18. F. Besenbacher, J.U. Andersen, E. Bonderup, Nucl. Instr. Meth. **168**, 1 (1980)
19. W.H. Barkas, W. Birnbaum, F.M. Smith, Phys. Rev. **101**, 778 (1956)
20. S.P. Møller, E. Uggerhøj, H. Bluhme, H. Knudsen, U. Mikkelsen, K. Paludan, E. Morenzoni, Phys. Rev. A **56**, 2930 (1997)
21. P. Sigmund, A. Schinner, Eur. Phys. J. D **12**, 425 (2000)
22. P. Sigmund, A. Schinner, Eur. Phys. J. D **15**, 165 (2001)
23. P. Sigmund, A. Schinner, Nucl. Instr. Meth. B **193**, 49 (2002)
24. P. Sigmund, A. Schinner, Nucl. Instr. Meth. B **212**, 110 (2003)
25. H.H. Andersen, A. Csete, T. Ichioka, H. Knudsen, S.P. Møller, U.I. Uggerhøj, Nucl. Instr. Meth. B **194**, 217 (2002)
26. U.I. Uggerhøj, H. Bluhme, H. Knudsen, S.P. Møller, E. Uggerhøj, E. Morenzoni, C. Scheidenberger, Nucl. Instr. Meth. B **207**, 402 (2003)
27. G. Hobler, K.K. Bourdelle, T. Akatsu, Nucl. Instr. Meth. B **242**, 617 (2006)
28. N. Wang, J.M. Pitarke, Phys. Rev. A **57**, 4053 (1998)